New approach for piezoelectric resonances and phase transitions in KDP and ADP crystals

2008 J. Phys.: Condens. Matter 20 465217

(http://iopscience.iop.org/0953-8984/20/46/465217)

IOP Publishing Journal of Physics: Condensed Matter

J. Phys.: Condens. Matter **20** (2008) 465217 (5pp) doi:10.1088/0953-8984/20/46/465217

New approach for piezoelectric resonances and phase transitions in KDP and ADP crystals

D P Pereira[1], P C de Oliveira[2], J Del Nero[3,4], P Alcantara Jr[3], C M R Remédios[3] and S G C Moreira[3]

[1] Centro Federal de Educação Tecnológica do Pará, 66093-020, Belém, Pará, Brazil
[2] Departamento de Física, Universidade Federal da Paraíba, 58051-970, João Pessoa, Paraíba, Brazil
[3] Departamento de Física, Universidade Federal do Pará, 66075-110, Belém, Pará, Brazil
[4] Instituto de Física, Universidade Federal do Rio de Janeiro, 21941-972, Rio de Janeiro, RJ, Brazil

Received 27 June 2008, in final form 18 September 2008
Published 21 October 2008
Online at stacks.iop.org/JPhysCM/20/465217

Abstract

In this work we introduce a new experimental setup, called here the three-electrode system (TES), which is very useful for analyzing and comparing piezoelectric crystals, as well as for studying their phase transitions and measuring their piezoelectric coefficients. ADP and KDP, which are very well-known crystals, were used in this work as good examples of piezo-crystals. The principal characteristic of TES is the application of an electric field to a small region of the crystal and the observation of the electric field at another region, usually located at the extremes of the crystal. In this way we can see several interesting effects, like piezoelectric resonances, phase transitions and harmonic generation, which are dependent on voltage and frequency conditions. We consider the piezoelectric concept in developing a mathematical model for the generated elastic wave, starting at the excitation electrode and traveling to the second electrode, where the signal depends on the piezoelectric coefficient. Our results have shown that this technique is very efficient for the determination of phase transitions.

1. Introduction

Piezoelectric crystals have been thoroughly investigated for more than 120 years, mainly for their actuator and sensor applications. At room temperature both KDP and ADP crystals are piezoelectric and their structure is tetragonal with $\bar{4}2m$ symmetry. The field of applicability is really very vast for this class of materials [1]. Studies of the propagation of signals through piezoelectric crystals have been developed under different experimental configurations [2, 3]. Some of these studies consider only two electrodes and others three electrodes [4, 5].

In 1945 Mason [6] measured elastic, piezoelectric and dielectric properties of KDP and ADP at temperatures above the Curie point (122 K or −151 °C). The piezoelectric properties were explained by a phenomenological theory by Mueller [7]. Bantle and Caflisch, according to the citation of Lang [8], performed a detailed description of direct piezoelectric effect measurements for the KDP crystal from room temperature up to the Curie point. Still according to Lang [8], Von Arx and Bantle used an interferometric technique to find the inverse piezoelectric effect, under the same temperature interval; this agreed with the direct piezoelectric effect, showing that the piezoelectric modulus has the same value for both effects, as described by Nye [9]. Nowadays, new techniques such as the multiple x-ray diffraction [10, 11] have been employed to determine the piezoelectric moduli of piezoelectric crystals.

In 1977 the first piezoelectric voltage transformer [12] was built. This could be applied in small electronic circuits where a traditional inductive transformer cannot be used. This kind of device was built using a setup similar to the one presented in this paper. Theoretical studies of electromagnetic wave propagation in piezoelectric crystals have already been developed [13, 14].

Also, classical works showing frequency filter crystals could be explained in terms of existing elastic wave theory and a cut-off frequency, where this effect confines the vibratory

energy to a limited region surrounding the electrode portion. For values lower than the cut-off frequency, the vibratory energy shows exponential behavior with distance of the electrode [15–17].

Generally, the properties of piezoelectric crystals are defined by their piezoelectric coefficients, where the crystal symmetry is one of the most important aspects [9]. These coefficients are specific to each crystal and are temperature [18] and pressure (uniaxial or hydrostatic) dependent. Many authors have characterized phase transitions by piezoelectric properties, since these properties may present anomalous behavior or discontinuities related to the phase transitions [19–23].

In this work we report on the characterization of the phase transitions of ADP and KDP crystals by their piezoelectric resonances, using the three-electrode system (TES). At room temperature both KDP and ADP crystals are piezoelectric (for KDP $d_{36} = 21 \times 10^{-12}$ C N^{-1} and for ADP $d_{36} = 52 \times 10^{-12}$ C N^{-1}), and they have a tetragonal structure with $\bar{4}2m$ symmetry. This latter property has been thoroughly investigated [8, 9] and it offers a good example for our measurements as well as the proposed model.

2. Experimental details

The crystals used in this work were grown by a low evaporation method, starting from a supersaturated solution at constant temperature (35 ± 0.3 °C). After the crystals were formed the samples were cut and polished in the shape of a parallelepiped plate of 5 × 3 × 0.4 mm^3, and the electrodes were painted with silver tin on [001] on both faces according to figure 1. In this way we have an input electrode (electrode 1), an output electrode (electrode 2) and a ground electrode (electrode 3).

We excited the piezoelectric sample using a lock-in amplifier (EG&G model 5302) and the frequency was scanned from 10 kHz up to 500 kHz with 5 V peak-to-peak amplitude. The generated signal at output electrode 2 was connected to the lock-in input channel.

We performed two kinds of experiments: one at constant temperature, scanning the frequency, and the other at constant frequency while the temperature was varied. For the experiments at constant frequency the sample was placed into a cryostat and the temperature was controlled from −196 °C up to 27 °C.

3. Theoretical modeling

The propagation of a mechanical wave in a crystal follows specific rules that depend on the elastic and piezoelectric properties of the crystal, and such a wave is accompanied by an electric field through piezoelectric coupling. Because the electric field is associated with the sound it is necessary to take electrical conditions into account. The elastic equation of motion is

$$\rho \frac{\partial^2 \mu_i}{\partial t^2} = \frac{\partial \sigma_{ij}}{\partial x_j}. \tag{1}$$

It is convenient to take the boundary conditions: $\mu(0,0) = \mu(0,L) = 0$ and $\sigma(0,0) = \sigma(0,L) = 0$, where L is sample length, μ_i are the components of the displacement vector and ρ is the mass density. This set of equations can assume different forms, depending on which parameters are fixed or controlled and also on the symmetries of the crystal. In our case, having strain ε and electric field E as controlled variables, we can write [24]

$$\begin{aligned} \sigma_{ij} &= C_{ijkl}\varepsilon_{kl} - C_{ijkl}d_{mij}E_m \\ D_n &= d_{nkl}\varepsilon_{kl} + \in_{nm} E_m \end{aligned} \tag{2}$$

where ε_{kl} is the strain tensor component, d_{mij} is the piezoelectric coefficient, $\in_{nm}$ is the dielectric constant, σ_{ij} is the stress tensor component, C_{ijkl} is the elastic constant, E_m is the electric field amplitude and D_n is the electric displacement.

A solution for equation (2) can be written as a plane wave $\mu = \mu_0 \cdot e^{-i(\omega t - \vec{k}\cdot\vec{r})}$, where $\vec{k}$ is the wavevector, ω is the angular frequency and μ_0 is the wave amplitude.

Considering a 45° cut and symmetry specific conditions for KDP and ADP crystals, with an electric field applied on [001] direction, we have

$$\begin{aligned} \sigma_1 &= C_{11}\varepsilon_1 + C_{12}\varepsilon_2 + C_{13}\varepsilon_3 = 0 \\ \sigma_2 &= C_{22}\varepsilon_2 + C_{23}\varepsilon_3 = 0 \\ \sigma_3 &= C_{33}\varepsilon_3 = 0 \\ \sigma_4 &= C_{44}\varepsilon_4 = 0 \\ \sigma_5 &= C_{55}\varepsilon_5 = 0 \\ \sigma_1 &= C_{66}\varepsilon_6 - C_{66}d_{36}E_3. \end{aligned} \tag{3}$$

Consequently,

$$\rho_S \frac{\partial^2 \mu_6}{\partial t^2} = \frac{C_{66}\mu_6}{L} - C_{66}d_{36}E_3 \tag{4}$$

where $\rho_S = \rho L$.

This equation completely describes wave propagation in our system.

Considering the experimental setup, we can divide the samples into two regions, as shown in figure 2. Region 1 comprises all crystal parts under electrode 1. This region of the crystal is excited by an electric field, given by $E_3 = E_1^0 \cos(\omega t)$, in the [001] direction and will vibrate with an amplitude μ_1. The remaining region of the crystal, despite there being no direct field action on it, is driven to vibrate because of the mechanical perturbation of the crystal lattice in addition to the piezoelectric effect. However, the amplitude in this part will be damped as a function of the distance of

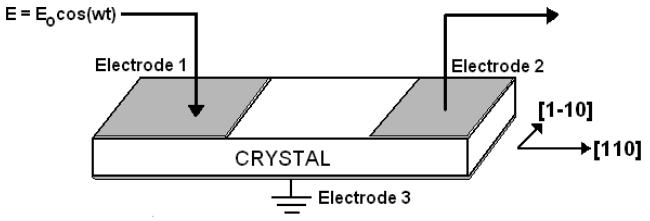

Figure 1. The three-electrode system. The dashed areas are the silvered regions.

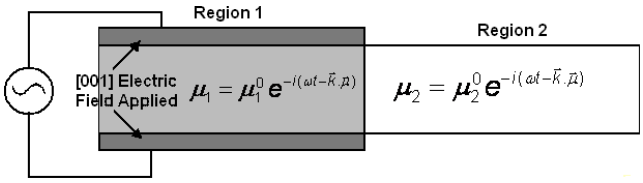

Figure 2. Showing two regions: region 1 with an applied electric field with solution (5) and region 2 without an electric field with solution (6).

propagation. Then, considering $\mu_{6(1)} = \mu_1$ and $\mu_{6(2)} = \mu_2$ as the deformations in the two regions, respectively, we have

$$\mu_1 = \mu_1^0 \cdot e^{-i(\omega t - \vec{k}\cdot\vec{\mu})} \tag{5}$$

$$\mu_1 = \mu_2^0 \cdot e^{-i(\omega t - \vec{k}\cdot\vec{\mu})}. \tag{6}$$

In figure 2 each solution, (5) and (6), is indicated in the two different regions. Equation (5) is the solution for region 1 while (6) is the solution for region 2.

Considering equations (5) and (6), equation (4) becomes

$$\begin{aligned} \rho_S \frac{\partial^2 \mu_1}{\partial t^2} &= \frac{C_{66}\mu_1}{L} + \frac{C_{66}\mu_2}{L} - C_{66} d_{36} E_3 \\ \rho_S \frac{\partial^2 \mu_1}{\partial t^2} &= -\frac{C_{66}\mu_1}{L} - \frac{C_{66}\mu_2}{L}. \end{aligned} \tag{7}$$

The solutions for the two regions have amplitudes μ_1^0 and μ_2^0, respectively, given by

$$\mu_1^0 = \left(\frac{\rho\omega^2 L - C_{66}}{\rho^2 \omega^4 L^3} \right) C_{66} d_{36} E_1^0 \tag{8a}$$

$$\mu_2^0 = \frac{C_{66}^2}{\rho^2 \omega^4 L^3} e^{-\alpha l} d_{36} E_1^0 \tag{8b}$$

where α is mechanical wave attenuation coefficient and l is the distance between the electrodes. We need to introduce a dissipation factor that is observed in experiments. This dissipative term arises when we consider the elastic constant C_{66} and the dielectric constant χ_3 as complex numbers. In this case, a exponential decay $\exp(-\alpha l)$ for amplitude (equation (8*b*)) naturally appears.

The electric field amplitude in electrode 2 is [25]

$$E_2^0 = 4\pi P_3 \text{ (CGS units)} \tag{9}$$

where P_3 is polarization in region 2 with direction [001]. Using the direct piezoelectric relation, we have

$$P_3 = d_{36}\sigma_6. \tag{10}$$

Taking into account also Hooke's law and equation (8*b*), we obtain the voltage in electrode 2:

$$V_2^0 = \frac{4\pi}{\rho^2\omega^4 L^4} C_{66}^3 d_{36}^2 e^{-\alpha l} V_1^0. \tag{11}$$

Introducing the relation $\chi_3 = d_{36}^2 C_{66}$ [8]:

$$V_2^0 = \frac{4\pi}{\rho^2\omega^4 L^4} \chi_3 C_{66}^2 e^{-\alpha l} V_1^0. \tag{12}$$

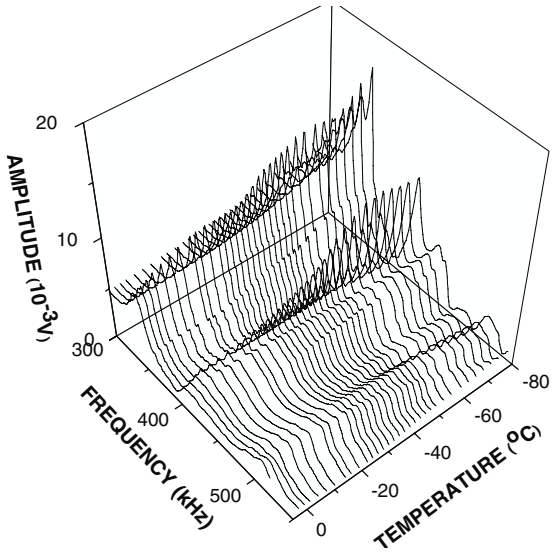

Figure 3. 3D graphic showing resonance spectra taken at different temperatures for the ADP crystal, where there is no evidence of phase transition.

The results (11) and (12) show that the voltage in output electrode (V_2^0) is dependent on the following parameters: the voltage in the input electrode (V_1^0), the piezoelectric coefficient (d_{36}), the elastic constant (C_{66}) (or the electric susceptibility (χ_3) and the constant (C_{66})) and decay exponentially with the distance between the electrodes (l). All these dependences were experimentally observed in our measurements.

4. Results and discussions

4.1. ADP crystal

Figure 3 shows the three-dimensional experimental data set of the piezoelectric resonance spectra (PRS) from −80 to 5 °C. These spectra were generated when we collect the output signal as a function of the excitation frequency. Figure 3 also shows that when the temperature is lowered the output signal becomes stronger for all frequencies.

This behavior for ADP crystal had already been reported by Mason [6], and it is a direct consequence of the decrease of d_{36} with temperature. According to equation (11) the output amplitude V_2^0 is directly dependent on $(d_{36})^2$. We can also see, around 320 and 400 Hz, that some frequency splitting arises. Such splitting can be explained by the breaking of the degenerate acoustic mode, therefore ADP crystal belongs to the $\bar{4}2m$ symmetry group with E (double degenerate mode). Other techniques, like Raman spectroscopy, show the same splitting behavior as a function of temperature [26]. Furthermore, the temperature effect always leads to linewidth narrowing and an increase in the intensity. Another interesting observation is the resonance frequency shift as a function of the temperature [27, 28]. This resonance frequency shift is more evident at high temperatures.

The strongest resonance is at $f = 260.2$ kHz. This fundamental resonance frequency was used to evaluate the

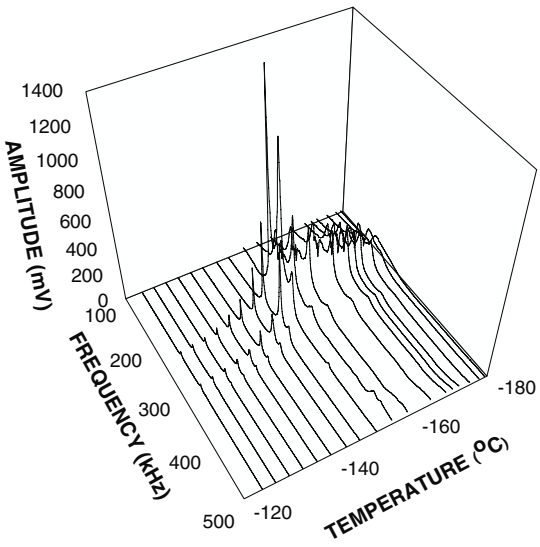

Figure 4. 3D graphic showing resonance spectra taken at different temperatures for the KDP crystal; the phase transition to −151 °C can be seen.

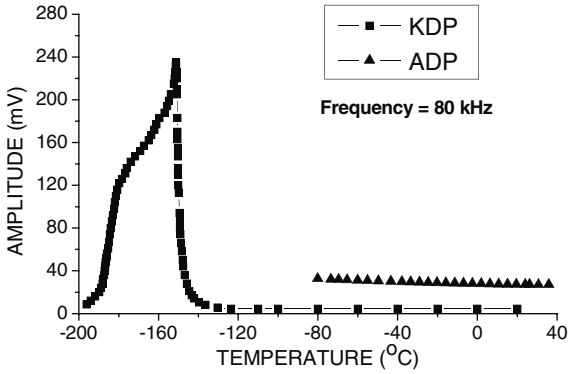

Figure 5. Temperature dependence of the field amplitude in electrode 2, where we can see the phase transition temperature of the KDP crystal. The frequency was constant at 80 kHz. ■ (KDP) and ▲ (ADP).

elastic compliance S_{66} through equation [29]:

$$f = \frac{1}{2l\sqrt{\rho S_{66}}},$$

where l is distance between electrodes and S_{66} is the elastic compliance constant (the elastic constant is the inverse of $S_{66} = 1/C_{66}$).

The value found value was:

$$S_{66} = \frac{1}{4l^2\rho f^2} = 16.9 \times 10^{-12}\ \text{cm}^2\ \text{dyn}^{-1}.$$

This value is in complete agreement with the literature value [30].

4.2. KDP results

Figure 4 shows a three-dimensional experimental data set for the PRS from −200 to −120 °C for KDP crystal using TES. In this figure we can see the evolution of PRS as a function of the temperature. The PRS shows different qualitative and quantitative characteristics for each phase below and above the phase transition temperature (−151 °C). Therefore, the PRS obtained with the experimental setup presented in this paper may be used to monitor a phase transition. Similar to other spectroscopic techniques, the PRS is related to the vibrational acoustic modes because the obtained spectra are generated basically by an electric field applied on the piezo-material generating a mechanical wave propagated from electrode 1 to electrode 2. Evidently, the strain and stress produced inside the sample are symmetry dependent, and any modification of the elastic parameter, like a phase transition, must reflect on the output signal (and consequently on PRS). For the case of KDP crystal, the well-known ferroelectric phase transition at −151 °C can be seen by the modified PRS figure 3. The main points in the figure are: (a) increase in spectral intensity around $T_c = -151$ °C; (b) a characteristic piezoelectric resonance spectrum for each phase of the crystal (paraelectric or ferroelectric).

Table 1. Obtained values of constants C_{66} and d_{36} for ADP and KDP crystals.

	Present paper		Other authors	
Crystal	C_{66} (dyn cm^{-2})	d_{36} (pC N^{-1})	C_{66} (dyn cm^{-2}) [30]	d_{36} (pC N^{-1}) [6]
ADP	5.9×10^{10}	52	6.02×10^{10}	51.7
KDP	6.02×10^{10}	20.5	6.25×10^{10}	21

For our experimental setup and taking into account the resonant frequency at $f = 171$ kHz and density $\rho = 2.332$ g cm^{-3} for KDP, we obtain the elastic compliance S_{66}:

$$S_{66} = \frac{1}{4l^2\rho f^2} = 1.66 \times 10^{-11}\ \text{cm}^2\ \text{dyn}^{-1}.$$

This result is in complete agreement with the literature [30–32].

Table 1 summarizes the data for (C_{66} and d_{36}) evaluated with equation (11), at room temperature. Those values have been compared with the literature values.

Another important result is that there is a temperature and frequency where the observed output signal is stronger than the input signal. For example, at −151 °C an output of 1400 mV was observed when the input signal was just 1000 mV. This represents a 40% increase in the input signal. Other authors [33, 34] have already shown the piezo-transformer effect but they used a different setup to observe it.

In a further exploration of the three-electrode system we also maintained the frequency constant at $f = 80$ Hz and scanned the temperature between $T_1 = -200$ °C and $T_2 = 40$ °C to observe the behavior of the output signal. Figure 5 shows the curves for the studied crystals. Although it is a very simple experiment, it presents an interesting result because it contains the thermal-elastic behavior of the crystal. Furthermore, it is possible to see a phase transition happening because the elastic and piezo-thermal properties affect the output signal, as we demonstrated in equations (11) and (12).

5. Conclusion

We introduced a new experimental setup, called here the three-electrode system (TES). Such a system has permitted us to analyze and measure the piezoelectric resonances on piezoelectric crystals such as ADP and KDP. Using such a simple system we observed the phase transitions undergone by crystals. The experimental setup is relatively simple, easy to work and provides a new way to test the piezoelectricity in crystals, ceramics or on any piezoelectric materials. Furthermore, the experimental setup was very sensitive in verifying the occurrence of phase transitions in the tested samples. We developed a theoretical model to evaluate, through TES, the piezoelectric moduli for ADP and KDP crystals using a very simple methodology.

Acknowledgments

PAJr, and CMRR are grateful to CNPq and FAPESPA. JDN would like to thank FAPERJ, FAPESPA and CAPES-DAAD for financial support. SGCM and DPP would like to thank CNPq and CAPES for financial support.

References

[1] Galassi C, Dinescu M, Uchino K and Sayer M (ed) 2000 *Piezoelectric Materials, Advances in Science, Technology and Applications* (*NATO Science Series: 3 High Technology* vol 76) (Dordrecht: Kluwer) pp 24–7
[2] Harvey A P and Tupholme G E 1992 *Wave Motion* **16** 125–35
[3] Wakatsuki N, Mizutani K and Nagai K 1995 *Japan. J. Appl. Phys.* **34** 2561–4
[4] Hamagami J, Hasegawa K and Kanamura K 2006 *Key Eng. Mater.* **320** 171–4
[5] Ye M, Wang B and Sato S 2006 *Opt. Commun.* **259** 710–22
[6] Mason W P 1946 *Phys. Rev.* **69** 173–94
[7] Muller H 1940 *Phys. Rev.* **57** 829
[8] Lang S B 1987 *Ferroelectrics* **71** 225–45
[9] Nye J F 2000 *Physical Properties of Crystals: Their Representation by Tensors and Matrices* (Oxford: Oxford University Press) pp 110–29
[10] dos Santos A O *et al* 2001 *J. Phys.: Condens. Matter* **13** 10497–505
[11] dos Santos A O, Cardoso L P, Sasaki J M, Miranda M A R and Melo F E A 2003 *J. Phys.: Condens. Matter* **15** 7835–42
[12] Igumnov D V, Gromov I S and Frolov V N 1977 *Telecommun. Radio Eng.* **31/32** 135–7
[13] Gufan A Y *et al* 2006 *Phys. Solid State* **48** 348–53
[14] Borrelli A, Horgan C O and Patria M C 2006 *Int. J. Solids Struct.* **43** 943–56
[15] Shockley W, Curran D R and Koneval D J 1963 *Proc. Frequency Control Symp.* pp 88–126
[16] Tiersten H F 1976 *J. Acoust. Soc. Am.* **59** 879–88
[17] Reilly N H C and Redwood M 1969 *Proc. IEE* **116** 653–60
[18] Meier W and Finkelmann H 1993 *Macromolecules* **26** 1811–7
[19] Budimir M, Damjanovic D and Setter N 2003 *J. Appl. Phys.* **94** 6753–61
[20] Guo Y P *et al* 2003 *J. Inorg. Mater.* **18** 220–4
[21] Guo Y P *et al* 2003 *J. Phys.: Condens. Matter* **15** L77–82
[22] Straube U and Beige H 2000 *J. Alloys Compounds* **310** 181–3
[23] Masuda S and Akishige Y 1998 *J. Korean Phys. Soc.* 2 **32** (Suppl. S) S783–5
[24] Ikeda T 1997 *Fundamentals of Piezoelectricity, Oxford Science Publications* (New York: Oxford University Press) (Corrected edn)
[25] Kittel C 2004 *Introduction to Solid State Physics* 8th edn (New York: Wiley)
[26] Arefev I M and Bazhulin P A 1965 *Sov. Phys.—Solid State USSR* **7** 326
[27] Mavrin B N *et al* 2006 *Opt. Spectrosc.* **100** 862–8
[28] Kudo K *et al* 2005 *Ferroelectrics* **323** 157–64
[29] Takagi T *et al* 2005 *Key Eng. Mater.* **301** 15–8
[30] Fritz I J 1976 *Phys. Rev.* B **13** 705–12
[31] Garland C W and Novotny D B 1969 *Phys. Rev.* **177** 971
[32] Maeda M *et al* 1991 *Japan. J. Appl. Phys.* 1 **30** 2394–7
[33] Wakatsuki N, Ueda M and Satoh M 1993 *Japan. J. Appl. Phys.* **32** 2317–20
[34] Karlash V L 2004 *J. Sound Vib.* **277** 353–67